



# Assessment of chemical stability of monoclonal antibody and antibody drug conjugate administered by pressurized intraperitoneal aerosol chemotherapy

Valentina D'Atri<sup>a,b</sup>, Guillaume Galy<sup>c</sup>, Mathias Buff<sup>a,b</sup>, Mateusz Imiolek<sup>d</sup>, Martin Hübner<sup>e</sup>,  
Manuela Undurraga<sup>f</sup>, Sana Intidhar Labidi-Galy<sup>g,h</sup>, Davy Guillaume<sup>a,b,\*</sup>, Laurent Carrez<sup>c</sup>

<sup>a</sup> School of Pharmaceutical Sciences, University of Geneva, CMU, Rue Michel Servet 1, Geneva 1211, Switzerland

<sup>b</sup> Institute of Pharmaceutical Sciences of Western Switzerland, University of Geneva, CMU, Rue Michel Servet 1, Geneva 1211, Switzerland

<sup>c</sup> Pharmacy, Lausanne University Hospital (CHUV), Lausanne, Switzerland

<sup>d</sup> Waters Corporation, Geneva 1211, Switzerland

<sup>e</sup> Visceral Surgery, Lausanne University Hospital (CHUV), University of Lausanne (UNIL), Switzerland

<sup>f</sup> Division of Gynecology, Department of Pediatrics and Gynecology, Hôpitaux Universitaires de Genève, Genève, Switzerland

<sup>g</sup> Department of Oncology, Hôpitaux Universitaires de Genève, Genève, Switzerland

<sup>h</sup> Faculty of Medicine, Department of Medicine and Center of Translational Research in Onco-Hematology, University of Geneva, Swiss Cancer Center Leman, Genève, Switzerland

## ARTICLE INFO

### Keywords:

Pressurized intra-peritoneal aerosol chemotherapy  
PIPAC  
Pembrolizumab Keytruda®  
Trastuzumab-deruxtecan enhertu®  
Stability  
antibody drug conjugate  
drug to antibody ratio

## ABSTRACT

Pressurized intraperitoneal aerosol chemotherapy (PIPAC) is a new therapeutic approach for patients with peritoneal cancer. So far, most published studies investigated the administration of established cytostatic agents through PIPAC. This study aimed to evaluate the effect of PIPAC on two breakthrough anti-cancer agents, specifically anti-PD1 pembrolizumab, and anti-HER2 antibody-drug conjugate (ADC) - trastuzumab-deruxtecan. We conducted systematic analyses on samples of pembrolizumab and trastuzumab-deruxtecan at clinically relevant concentrations before and after PIPAC administration using an experimental setup of a hermetic container system, mimicking the abdominal cavity and using identical features as in clinical use. We utilized a range of chromatographic and spectroscopic techniques to explore potential alterations in the primary, secondary, and tertiary structures of the drugs, focusing on post-translational modifications resulting from the aerosolization. Our findings indicate that PIPAC did not compromise the integrity of tested biopharmaceuticals. The size variants of both drugs, assessed by size exclusion chromatography (SEC), remained unchanged. Reversed-phase liquid chromatography (RPLC) and hydrophobic interaction chromatography (HIC) revealed no significant differences in hydrophobicity variants, the average drug-to-antibody ratio (DAR), or DAR distribution before and after PIPAC treatment. Circular dichroism (CD) spectroscopy confirmed that the secondary and tertiary structures were preserved. While pembrolizumab showed no change in charge variants post-PIPAC, trastuzumab-deruxtecan exhibited a non-negligible change in the quantity of charge variants on the monoclonal antibody itself, while the payload remained unchanged. This shift could possibly be related to the metallic composition of the CapnoPen® device (made of nickel and chromium) used in PIPAC and for these experiments. Together, our results suggest that PIPAC does not alter the structure of pembrolizumab and trastuzumab-deruxtecan, paving the way for future clinical trials.

## 1. Introduction

Peritoneal metastases are a major therapeutic challenge for several gastrointestinal and gynaecological cancer types. There are few

therapeutic options for these patients that ultimately develop life-threatening complications such as ileus, refractory malignant ascites and bowel perforation [1]. Pressurized intraperitoneal aerosol chemotherapy (PIPAC) is a laparoscopic procedure for intraperitoneal (IP)

\* Correspondence to: Institute of Pharmaceutical Sciences of Western Switzerland (ISPSO), School of Pharmaceutical Sciences, University of Geneva, CMU, Rue Michel Servet 1, Geneva 1211, Switzerland.

E-mail address: [davy.guillaume@unige.ch](mailto:davy.guillaume@unige.ch) (D. Guillaume).

<https://doi.org/10.1016/j.jpba.2024.116410>

Received 26 June 2024; Received in revised form 9 August 2024; Accepted 10 August 2024

Available online 15 August 2024

0731-7085/© 2024 The Authors. Published by Elsevier B.V. This is an open access article under the CC BY license (<http://creativecommons.org/licenses/by/4.0/>).

administration of chemotherapy as an aerosol using a standardized high-pressure injector. It generates an artificial pressure gradient that enhances tissue drug uptake by convection and distributes drugs more homogeneously within the closed and expanded abdominal cavity. This route allows the administration of up to 10 times less chemotherapy drug than via IV, reducing systemic toxicity and potentially increasing intra-tumoral drug concentration [2]. Up to 3 PIPAC could be administered every 4–6 weeks to a patient with peritoneal carcinomatosis [2, 3].

In the last decade, two breakthrough therapies have led to dramatic improvement of patients survival in many cancers: immune checkpoint inhibitors (ICIs) [4] and antibody-drug conjugates (ADCs) [5]. ICIs, particularly monoclonal antibodies (mAbs) targeting Programmed-Death 1 (PD1)/PD-L1 are backbone therapy of multiple cancers such as melanoma, lung cancer and endometrial cancer. There is a dozen of approved ICIs that can be administered as a monotherapy or in combination with chemotherapy drugs and/or target therapies. PD1 is expressed at the surface of T cells, while its ligand anti-PD-L1 is expressed by tumor cells and/or antigen-presenting cells (myeloid cells). Abrogation of immune checkpoint signalling leads to reactivation of the immune system toward tumor cell killing. Anti-PD1 pembrolizumab is by far the most widely used cancer drug with approval in more than 30 indications [6]. On the other hand, ADCs combine the specificity of mAbs directed toward tumor-associated antigens, with highly potent cytotoxic agents (payload) attached through chemical linkers. The cytotoxic effect of the payload alone is generally very high, preventing its systemic administration. This targeted drug delivery aims to reduce off-target toxicities while maximizing on-target cytotoxicity. Until recently, the majority of approved ADCs had a drug-to-antibody (DAR) ratio of 3–4. Next-generation ADCs such as trastuzumab-deruxtecan and sacituzumab-govitecan that incorporate topoisomerase 1 inhibitors, had a DAR around 8, meaning that it is possible to deliver a higher number of cytotoxic molecules to each targeted tumor cell.

While the use of PIPAC has spread in the last years in Europe and is a therapeutic palliative option in numerous hospitals, only a few chemotherapy drugs (i.e. cisplatin, doxorubicin, oxaliplatin, nab-paclitaxel) have been tested for PIPAC administration within clinical trials. Importantly, the administration of breakthrough therapies such as ADCs and ICIs have not been yet tested by PIPAC. One major concern of PIPAC is that this alternative way of administration could potentially alter the structure and hence the anti-tumoral effect of mAbs. Another concern specific to ADCs is safety and whether PIPAC would detach payload from monoclonal antibodies.

To explore the impact of PIPAC on ICIs and ADCs used in the clinics, we focused on two extensively prescribed drugs: the ICI pembrolizumab, targeting PD1, and the ADC trastuzumab-deruxtecan, targeting HER2. Our study involved a thorough analysis of samples collected before and after PIPAC treatment. We employed a variety of chromatographic techniques, including size exclusion chromatography (SEC), cation exchange chromatography (CEX), reverse phase liquid chromatography (RPLC), and hydrophobic interaction chromatography (HIC), complemented by circular dichroism (CD) spectroscopy in both near and far UV ranges. These methods enabled us to detect and characterize potential degradation products that may form during PIPAC administration.

## 2. Materials and methods

### 2.1. Chemicals and reagents

Type 1 water was obtained from a Milli-Q™ purification system from Millipore (Bedford, MA, USA). LC-MS grade acetonitrile and methanol were purchased from Thermo Fisher Scientific (Reinach, Switzerland). Potassium chloride salt (>99.5 %), potassium phosphate monobasic (>99.5 %), potassium phosphate dibasic (>99.0 %), sodium chloride (>99.5 %), 2-(Nmorpholino)ethanesulfonic acid (MES) sodium salt,

MES monohydrate (>99.5 %), ammonium sulfate (>99.5 %), and trifluoroacetic acid (TFA, >99.0 %), were obtained from Sigma-Aldrich (Buchs, Switzerland). The pH of the mobile phase was adjusted with a SevenMulti S40 pH meter (Mettler Toledo, Greifensee, Switzerland). The monoclonal antibody (mAb) Keytruda™ (pembrolizumab 25 mg/mL, lot number X010907, expiring date 10/2024) and the antibody-drug conjugate (ADC) Enhertu™ (trastuzumab-deruxtecan 100 mg, lot number 386009, expiring date 08/2026) were obtained as European Union pharmaceutical-grade drug products from their respective manufacturer.

### 2.2. Description of the PIPAC experimental setup

All the experiments were performed in two steps, as described below.

#### Step 1: Preparation of syringes for PIPAC administration

Syringes of trastuzumab-deruxtecan and pembrolizumab for PIPAC usage were produced under an isolator in a class C environment. The compounding of chemotherapies was assisted by a production computer software BD Cato™ in volumetric method with visual double-check control, in a same way as routine production. Drugs were prepared in syringes ESL 200 mL by Medtron AG Germany. Pembrolizumab (2 mg/mL) was diluted in 50 mL 0.9 % NaCl. Trastuzumab-deruxtecan (0.5 mg/mL and 1 mg/mL) was diluted in 50 mL 5 % dextrose.

#### Step 2: Experimental setup of PIPAC

During PIPAC, chemotherapy drugs are injected, during a laparoscopic procedure, as an aerosol in the abdominal cavity of a patient using a standard high-pressure injector and the specific nebuliser (there are 4 devices currently available on the market, and we used one of them, as indicated below). In order to mimic the clinical conditions, an experimental PIPAC setup was built, in collaboration with a surgeon specialist having performed >500 PIPAC procedures before. For this purpose, a hermetic container system and the PIPAC device of clinical practice in the operating room were used, as shown in Fig. 1. The abdominal cavity was mimicked using a sterile bag of 3 L volume of 0.9 % NaCl (BBraun), made empty from NaCl. A new empty bag was used for each nebulisation of a new drug. The setup system was made hermetic by the open placement of one 10 mm balloon trocar into the empty bag. The Seal of the container was checked through zero flow of the CO<sub>2</sub> insufflator. The nebulizer was inserted via the trocar. The recommended device insertion angle of 57–66° was respected. All drugs were aerosolized using a pressure injector (Accutron™ injector HP-D Thera, Medtron Saarbrücken Germany) and a specific nebulizer (CapnoPen® device, Capno Pharm, Tübingen, Germany; CE-certified: class 2b) under standard laparoscopic pressure of 12 mm Hg of CO<sub>2</sub> by an insufflator. The minimally nebulized volume was 20 mL. One CapnoPen® device was used per molecule, and a rinse was performed with 5% dextrose between different concentrations of Trastuzumab-deruxtecan.

To keep the consistency of experimental conditions, all samples were collected at the operation room. Samples collected before PIPAC were extracted from the ESL syringes. Samples collected after PIPAC were extracted from the 3 L bag after drug nebulisation. All samples collected had a volume of 20 mL, collected using a 30 mL syringe (BD) using a spike (TAKE SET from CODAN companies) connected to the bag.

Samples were provided at different concentrations (Table 1) and directly analysed by liquid chromatography methods. For CD measurements, mAb and ADC samples were diluted to approximately 0.05 mg/mL in experimental buffers (namely 0.9 % NaCl and 5 % dextrose for pembrolizumab and trastuzumab-deruxtecan samples, respectively).

### 2.3. HPLC experiments

#### 2.3.1. Chromatographic system

Measurements were conducted using a Waters ACQUITY™ UPLC™ H-Class Bio System (Waters, Milford, MA, USA). This system includes a quaternary solvent delivery pump and an autosampler with a 15 µL flow-through needle (FTN) injector which used an 85/15 water/



**Fig. 1.** PIPAC simulation setup in the operation room. **A.** PIPAC setup in the operation room followed the same procedure than in clinical practice with a pressure injector (a), CO<sub>2</sub> laparoscopic insufflator (b) and an empty sterile bag (c). **B.** All drugs were aerosolized using a pressure injector and a specific nebulizer using ESL syringes. **C.** The abdomen was mimicked using an empty and sealed sterile bag of 3 L volume. The system was made hermetic by the open placement of one 10 mm balloon trocar in the empty bag.

**Table 1**

Summary of the results obtained in all chromatographic modes (SEC, SEC, RPLC and HIC) for the pembrolizumab at 2 mg/mL, before and after PIPAC.

<b>SEC</b>							
tr (min)	6.1	6.6					
Proportion of species before PIPAC	6.9 %	93.1 %					
%RSD area (3 replicates before PIPAC)	1.8 %	0.6 %					
Proportion of species after PIPAC	6.7 %	93.3 %					
%RSD area (3 replicates after PIPAC)	6.0 %	4.7 %					
Δ %Area before/after PIPAC (%)	-0.2 %	0.2 %					
<b>CEX</b>							
tr (min)	10.7	11.9	12.9				
Proportion of species before PIPAC	4.7 %	81.9 %	13.3 %				
%RSD area (3 replicates before PIPAC)	0.3 %	0.5 %	1.1 %				
Proportion of species after PIPAC	4.7 %	82.0 %	13.3 %				
%RSD area (3 replicates after PIPAC)	5.9 %	4.8 %	5.3 %				
Δ %Area before/after PIPAC (%)	0.0 %	0.0 %	0.0 %				
<b>RPLC</b>							
tr (min)	5.3	5.4	5.5	5.7			
Proportion of species before PIPAC	1.0 %	1.0 %	95.5 %	2.6 %			
%RSD area (3 replicates before PIPAC)	0.2 %	1.0 %	0.9 %	1.4 %			
Proportion of species after PIPAC	1.0 %	1.0 %	95.5 %	2.6 %			
%RSD area (3 replicates after PIPAC)	6.5 %	6.3 %	4.5 %	4.0 %			
Δ %Area before/after PIPAC (%)	0.0 %	0.0 %	0.0 %	0.0 %			
<b>HIC</b>							
tr (min)	13.3	16.3	18	18.9	21.1	22.8	23.6
Proportion of species before PIPAC	5.9 %	1.3 %	10.7 %	80.0 %	1.2 %	0.3 %	0.7 %
%RSD area (3 replicates before PIPAC)	3.0 %	0.3 %	0.7 %	0.9 %	0.7 %	1.7 %	1.0 %
Proportion of species after PIPAC	5.5 %	1.2 %	10.8 %	80.4 %	1.2 %	0.3 %	0.6 %
%RSD area (3 replicates after PIPAC)	5.0 %	2.8 %	4.2 %	4.2 %	4.1 %	2.8 %	3.9 %
Δ %Area before/after PIPAC (%)	-0.4 %	0.0 %	0.1 %	0.4 %	0.0 %	0.0 %	0.0 %

methanol mixture as the rinsing solvent. Additionally, it was equipped with a fluorescence (FL) detector that operated with an excitation at 280 nm and emission at 340 nm, a data acquisition rate of 5 Hz, time

constant of 2 s, and a 2 μL cell. All data acquisition, processing, and control of the instrument were managed through Empower™ Pro 3 Software.

### 2.3.2. SEC conditions

The experimental setup was adapted from a protocol recently published by our research group [7]. SEC analyses were performed on an AdvanceBio™ SEC PEEK lined column, 300 Å, 2.7 µm, 4.6 × 300 mm from Agilent Technologies (Wilmington, DE, USA). The mobile phase was composed of 50 mM potassium phosphate at pH 6.8 in the presence of 250 mM KCl. This solution was filtered through a 0.45 µm filter and applied isocratically at a flow rate of 0.4 mL/min at room temperature. For all SEC-FD experiments, the injection volume was consistently maintained at 5 µL.

### 2.3.3. CEX conditions

The experimental conditions were adapted from those detailed in a protocol paper recently published by our research group [7]. CEX analyses were conducted using a MABPac™ SCX-10 RS column, 5 µm, 4.6 × 50 mm from Thermo Fisher Scientific AG (Sunnyvale, CA, USA). Mobile phase A consists of 10 mM MES buffer at pH 6, and mobile phase B included the same buffer at pH 6 but with 1 M NaCl. The solution was filtered through a 0.45 µm filter and delivered in a gradient mode following this sequence: a gradient from 0 % to 20 % B over 20 min, a sharp increase from 20 % to 100 % B in 0.1 min, maintained at 100 % B for 1 minute, quickly returned to 0 % B in 0.1 min, and then re-equilibrated for 9 min. The total analysis time was 30 min. The flow rate was maintained at 0.4 mL/min at room temperature. A consistent injection volume of 5 µL was used for all CEX-FD experiments.

### 2.3.4. RPLC conditions

RPLC analyses were performed using a BioResolve™ Polyphenyl Column, 450 Å, 2.7 µm, 2.1 × 150 mm, from Waters. Mobile phase A was composed of 0.1 % TFA in water, and mobile phase B included acetonitrile (ACN) with 0.1 % TFA. The mobile phases were filtered through a 0.45 µm filter and delivered using a gradient program: increasing from 27 % to 56 % B over 12 min, then rapidly decreasing to 27 % B in 0.1 minute, followed by a 6-minute equilibration period. The total analysis time was 18 min. The flow rate was set at 0.4 mL/min, and the experiments were carried out at 80 °C. For all RPLC-FD experiments, the injection volume was consistently equal to 1 µL.

### 2.3.5. HIC conditions

The experimental conditions were adapted from those detailed in a protocol paper recently published by our research group [7]. HIC analyses utilized a MABPac HIC-10 column, 1000 Å, 5 µm, 4.6 × 250 mm from Thermo Fisher Scientific AG. Mobile phase A included 100 mM potassium phosphate at pH 6.8 with 1 M ammonium sulfate, and mobile phase B consisted of 100 mM potassium phosphate at pH 6.8 alone. The mobile phases were filtered through a 0.45 µm filter and applied using a gradient program: from 0 % to 100 % B over 40 min, maintained isocratically at 100 % B for 5 min, quickly reduced to 0 % B in 0.1 minute, followed by a 15-minute re-equilibration period. The total analysis time was 60 min. The flow rate was maintained at 0.8 mL/min, and experiments were conducted at room temperature. An injection volume of 5 µL was consistently used for all HIC-FD experiments.

## 2.4. Circular dichroism (CD) experiments

The mAb samples were diluted in a 0.9 % NaCl solution (B. Braun 534534), and ADC samples were diluted in a 5 % dextrose solution (B. Braun 531032). For CD studies assessing secondary and tertiary structures, sample concentrations were set at 0.05 mg/mL for near UV-CD analysis for all samples, and 0.04 mg/mL for mAbs and 0.05 mg/mL for ADCs for far UV-CD. These analyses were conducted using a J-815 Circular Dichroism Spectrophotometer (JASCO, Easton, MD, USA), managed via Spectra Manager software. Tertiary structures were examined in the 250–350 nm range to identify CD peaks corresponding to tryptophan, tyrosine, and phenylalanine, alongside a broader signal from disulfide bonds between 250 and 280 nm. Secondary structures

were analyzed from 205 to 250 nm, focusing on signals indicative of  $\alpha$ -helices,  $\beta$ -sheets, turns, and random coils. Post-measurement, the data was processed using Spectra Manager software to perform baseline correction, and averages were derived from three spectral replicates per sample. Further analysis was carried out using Excel™ software.

## 3. Results and discussion

The results and discussion section is structured according to the type of post-translational modification (PTM) observed, including size variants, charge variants, hydrophobicity variants, and secondary/tertiary structures. For each PTM category, we tested two different samples - pembrolizumab and trastuzumab-deruxtecan - at two different, clinically relevant concentrations.

Pembrolizumab is currently administered in clinical routine at a flat dose of 200 mg IV every 3 weeks. Thus, we chose a dose of 2 mg/mL, which would correspond to a total amount of 200 mg for a 100 mL ESL syringe. On the other hand, Trastuzumab-deruxtecan is currently administered by IV at a dose of 6.4 mg/Kg for gastric cancer, corresponding to a total dose of 448 mg for a 70 kg patient. PIPAC route allows the administration of up to 10 times less chemotherapy drug than IV route, reducing systemic toxicity and potentially increasing intratumoral drug concentration. Here, we chose to test Trastuzumab-deruxtecan at a concentration of 0.5 mg/mL and 1 mg/mL, corresponding to a total dose of 50 and 100 mg, for 100 mL ESL syringe. For the future phase 1 trial of Trastuzumab-deruxtecan by PIPAC to be designed, 50 mg would be the first dose cohort, corresponding to 10 times lower dosage than IV route. All the experiments were performed in triplicate.

### 3.1. Analysis of size variants using SEC

Size variants of mAbs, typically around 150 kDa, include both smaller antibody fragments and larger aggregates. These variants can develop through the manufacturing process or during storage and are critical for the efficacy and safety of therapeutic mAbs. They are recognized as critical quality attributes (CQAs) that require thorough characterization. Aggregates are of particular concern because they can induce immunogenicity, potentially triggering adverse immune responses and diminishing the therapeutic effectiveness. Size variants are prone to formation under stress conditions such as temperature changes, UV light exposure, and agitation [8]. Consequently, it is essential to monitor fragments and aggregates during the administration of chemotherapy with PIPAC, especially as the treatment involves the use of a standard high-pressure injector that can create pressures as high as 20 bar, leading to the generation of aerosols. Of note, the droplet size of the aerosol is determined by the device and the upstream pressure which is indirectly determined by the flow rate of the high-pressure injector.

SEC is recognized as a benchmark method for assessing size variants of mAbs and related compounds, with substantial literature on the subject published in recent years [9–11]. In our current study, we employed a bioinert (PEEK-coated) column to minimize secondary interactions, such as ionic and hydrophobic interactions, as recently demonstrated [12,13]. Furthermore, we opted for a long column of 300 mm length, packed with small particles of 2.7 µm, to enhance separation efficiency and effectively separate aggregates and fragments. The mobile phase contains a relatively high concentration of KCl (250 mM), which has been reported to significantly reduce secondary ionic interactions [14].

Under the optimized SEC conditions, both pembrolizumab and trastuzumab-deruxtecan were successfully analyzed. The chromatograms from three replicates performed before and after the PIPAC treatment are presented in Figs. 2–4A, for pembrolizumab at 2 mg/mL and trastuzumab-deruxtecan at 0.5 and 1 mg/mL, respectively. The results showed no low molecular weight species (LMWS) in either sample. However, high molecular weight species (HMWS) were detected,

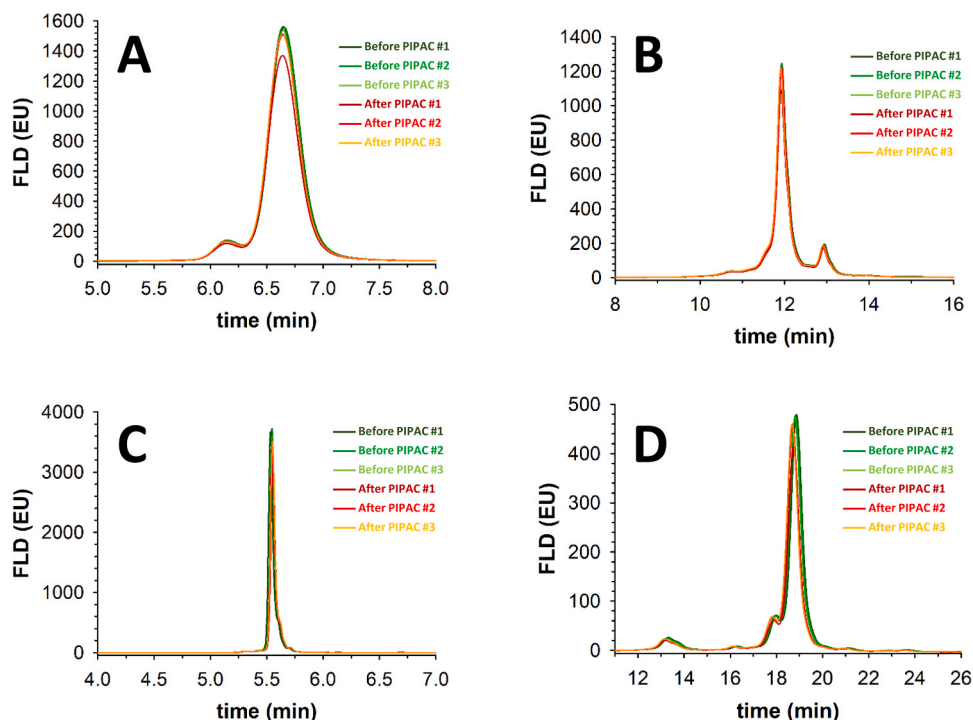


**Fig. 2.** Analysis of pembrolizumab at a concentration of 2 mg/mL in four different chromatographic modes. Six samples were analyzed, including three replicates before the PIPAC (Before PIPAC #1, #2 and #3) and 3 replicates after the PIPAC (After PIPAC #1, #2 and #3). (A) SEC mode, (B) CEX mode, (C) RPLC mode, (D) HIC mode.

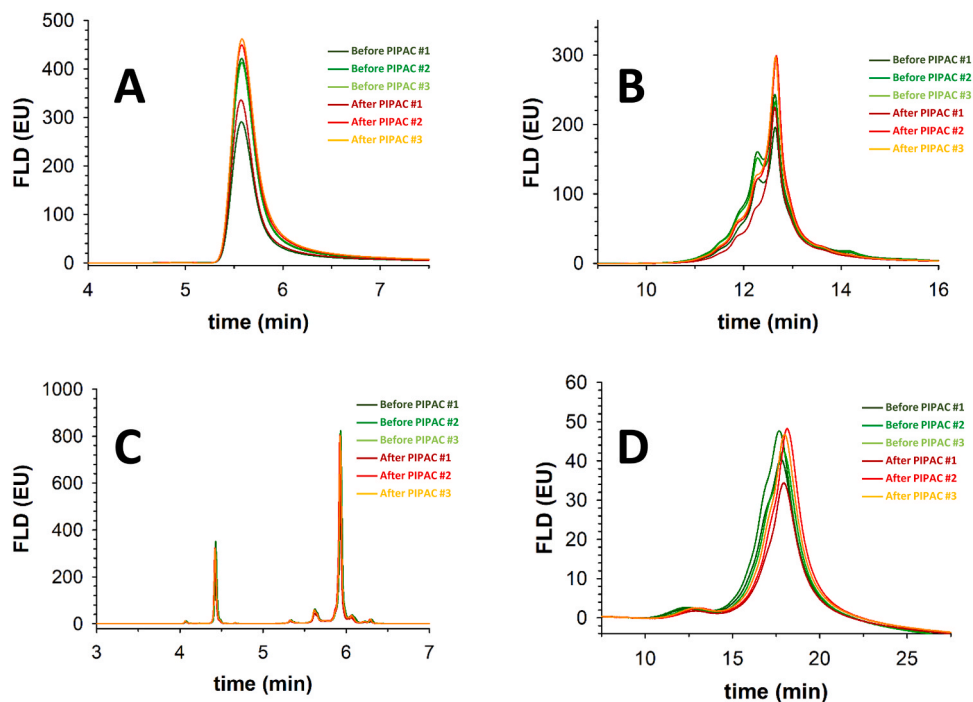


**Fig. 3.** Analysis of trastuzumab-deruxtecan at a concentration of 0.5 mg/mL in four different chromatographic modes. Six samples were analyzed, including three replicates before the PIPAC (Before PIPAC #1, #2 and #3) and 3 replicates after the PIPAC (After PIPAC #1, #2 and #3). (A) SEC mode, (B) CEX mode, (C) RPLC mode, (D) HIC mode.

constituting over 6 % of the pembrolizumab samples and less than 0.3 % of the trastuzumab-deruxtecan samples. Our previous research on pembrolizumab identified these HMWS as oxidation variants of the monomeric form, specifically with one or two oxidized methionine residues [15]. In contrast, the minor HMWS peak in the

trastuzumab-deruxtecan sample was confirmed to be a dimer, as previously established [16].

For the pembrolizumab sample at 2 mg/mL, the relative standard deviation (RSD) of the peak area across three replicates was 1.8 % before the use of PIPAC, which increased to 6.0 % after PIPAC treatment. This

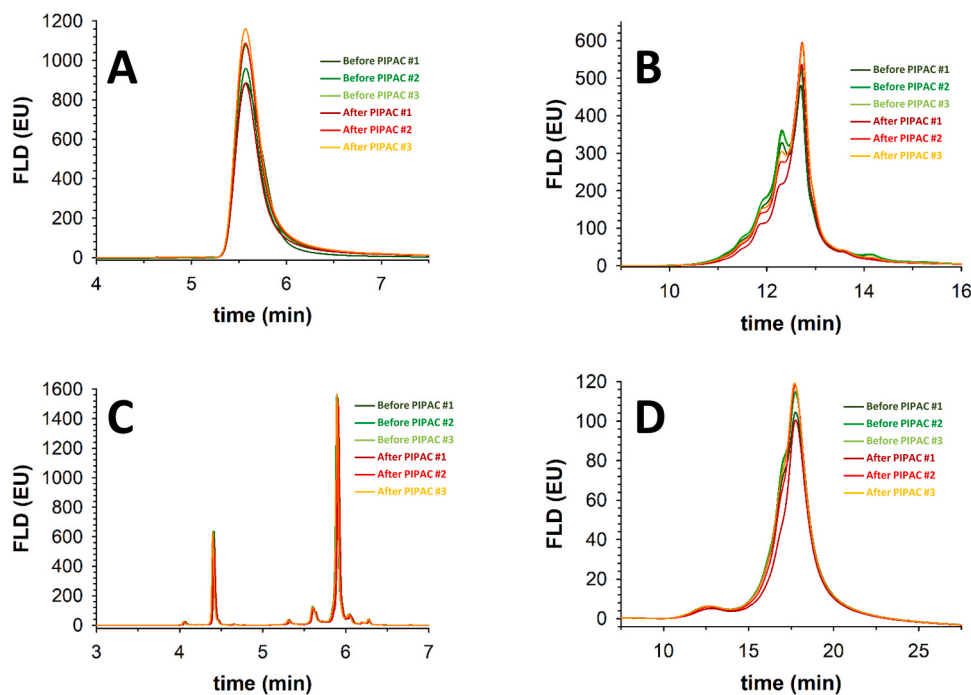


**Fig. 4.** Analysis of trastuzumab-deruxtecan at a concentration of 1 mg/mL in four different chromatographic modes. Six samples were analyzed, including three replicates before the PIPAC (Before PIPAC #1, #2 and #3) and 3 replicates after the PIPAC (After PIPAC #1, #2 and #3). (A) SEC mode, (B) CEX mode, (C) RPLC mode, (D) HIC mode.

increase in variability was anticipated due to the complexities involved in sample collection post-PIPAC, where some pembrolizumab molecules may adhere to the surface of the plastic bag used to simulate the stomach environment, resulting in greater variability. This pattern of increased variability post-PIPAC is always observed throughout this study, regardless of the chromatographic mode or the sample tested. In SEC, the proportion of HMWS in pembrolizumab, identified as oxidation variants, eluted at 6.1 min were 6.9 % and 6.7 % before and after PIPAC, respectively. For trastuzumab-deruxtecan, the amount of HMWS remained consistent (0.3 % before PIPAC and 0.2 % after PIPAC), regardless of the concentration. Given the variability between replicates, the differences observed before and after PIPAC are not statistically significant, indicating that PIPAC does not increase the amount of size variants nor does it induce chemical degradation in the two chemotherapy products.

### 3.2. Analysis of charge variants using CEX

Charge variants of mAbs represent another significant source of variability and have become an important aspect to consider within the biotechnology industry, due to their potential impact on stability and biological activity [17,18]. Common types of antibody charge variants include acidic variants such as those arising from sialylation, deamidation, and glycation, and basic variants, which may result from incomplete removal of C-terminal lysine, incomplete cyclization of N-terminal glutamine to pyroglutamate, succinimide formation, and isomerization of asparagine, among others, compared with the main species [19]. These charge variants may appear during the production or storage of mAb products or under various stress conditions [8].

Two analytical methods are commonly used for characterizing charge variants of mAbs: imaged capillary isoelectric focusing (icIEF) and cation exchange chromatography (CEX) [20]. Acidic and basic species are distinguished based on their elution times relative to the main peak in these techniques. Generally, there is a strong correlation, with only minor discrepancies, between the profiles and quantities of acidic and basic species detected by both methods. For this study, we

chose to use CEX to evaluate the charge variants of the two mAb-based products. In CEX, acidic variants are those that elute earlier than the main peak, while basic variants elute later than the main peak [21]. Employing a modern strong cation exchange (SCX) non-porous column with a salt gradient at pH 6, we produced the chromatograms shown in Figs. 2–4B. These figures present an overlay of six chromatograms, comprising three replicates both before and after PIPAC treatment.

In the case of pembrolizumab, the analysis clearly resolved at least one acidic variant, eluting at 10.7 min, and one basic variant, eluting at 12.9 min, from the main peak. The identification of acidic and basic variants aligns with previous studies documented in the literature [22]. According to the chromatograms displayed in Fig. 2B, the profiles of the six different pembrolizumab samples appear consistent. This observation is confirmed by the data presented in Table 1, where the proportions of acidic and basic variants were equal to 4.7 % and 13.3 %, respectively, both before and after PIPAC treatment, indicating no changes in the charge variant profile due to PIPAC. Furthermore, variability in peak areas for the three replicates before PIPAC ranged from 0.3 % to 1.1 %, while after PIPAC, it varied between 4.8 % and 5.9 %. This level of variability corresponds with earlier findings from the SEC analysis (see previous section).

Trastuzumab-deruxtecan exhibited greater heterogeneity, with only partial separation achieved for the acidic variants, as indicated in Figs. 3B and 4B. The same variants were observed before and after PIPAC, although there was a notable change in the relative amounts of these variants. This change is clearly outlined in Tables 2 and 3. For instance, at the lower concentration of 0.5 mg/mL, the proportion of acidic variants shifted from 39.3 % to 31.2 % post-PIPAC. At a higher concentration of 1 mg/mL, the percentages changed from 45.9 % to 36.6 %. The observed differences pre- and post-PIPAC are considered significant. In addition, the variability among the three replicates was significantly higher, reaching up to 18 % post-PIPAC, compared to the one observed with pembrolizumab. This increased variability is attributed to the challenging peak integration due to poor separation that is superimposed on the post-PIPAC sample collection issue previously described. To ensure that the differences observed before/after PIPAC

Table 2

Summary of the results obtained in all chromatographic modes (SEC, SEC, RPLC and HIC) for the trastuzumab Deruxtecan at 0.5 mg/mL, before and after PIPAC.

SEC						
tr (min)	4.9	5.6				
Proportion of species before PIPAC	0.3 %	99.7 %				
%RSD area (3 replicates before PIPAC)	7.5 %	16.6 %				
Proportion of species after PIPAC	0.2 %	99.8 %				
%RSD area (3 replicates after PIPAC)	16.8 %	16.2 %				
Δ %Area before/after PIPAC (%)	-0.1 %	0.1 %				
CEX						
tr (min)	12.3	12.6				
Proportion of species before PIPAC	39.3 %	60.7 %				
%RSD area (3 replicates before PIPAC)	15.4 %	6.6 %				
Proportion of species after PIPAC	31.2 %	68.8 %				
%RSD area (3 replicates after PIPAC)	18.4 %	12.3 %				
Δ %Area before/after PIPAC (%)	-8.1 %	8.1 %				
HIC						
tr (min)	12.4	17.8				
Proportion of species before PIPAC	5.4 %	94.6 %				
%RSD area (3 replicates before PIPAC)	4.3 %	5.6 %				
Proportion of species after PIPAC	5.4 %	94.6 %				
%RSD area (3 replicates after PIPAC)	9.0 %	12.1 %				
Δ %Area before/after PIPAC (%)	-0.1 %	0.1 %				
RPLC						
tr (min)	4.1	4.4	4.7	5.6	5.9	6.1
Proportion of species before PIPAC	1.5 %	18.8 %	0.4 %	12.1 %	59.2 %	8.0 %
%RSD area (3 replicates before PIPAC)	4.5 %	4.6 %	5.3 %	4.5 %	4.8 %	4.2 %
Proportion of species after PIPAC	1.5 %	18.9 %	0.4 %	11.9 %	59.8 %	7.5 %
%RSD area (3 replicates after PIPAC)	11.1 %	11.7 %	10.0 %	12.5 %	11.6 %	12.3 %
Δ %Area before/after PIPAC (%)	0.0 %	0.1 %	0.0 %	-0.1 %	0.6 %	-0.6 %

were not due to the poor separation quality in CEX for these samples, we developed an alternative method using a pH gradient with 20 mM MES adjusted to pH 5.6 for mobile phase A and 20 mM HEPES with 100 mM KCl adjusted to pH 8.2 for mobile phase B. This gradient was optimized and analysis time was extended (gradient from 40 % to 55 % B over

Table 3

Summary of the results obtained in all chromatographic modes (SEC, SEC, RPLC and HIC) for the trastuzumab Deruxtecan at 1 mg/mL, before and after PIPAC.

SEC						
tr (min)	4.9	5.6				
Proportion of species before PIPAC	0.3 %	99.7 %				
%RSD area (3 replicates before PIPAC)	4.5 %	6.3 %				
Proportion of species after PIPAC	0.2 %	99.8 %				
%RSD area (3 replicates after PIPAC)	12.6 %	11.2 %				
Δ %Area before/after PIPAC (%)	-0.1 %	0.1 %				
CEX						
tr (min)	12.3	12.7				
Proportion of species before PIPAC	45.9 %	54.1 %				
%RSD area (3 replicates before PIPAC)	4.7 %	3.4 %				
Proportion of species after PIPAC	36.6 %	63.4 %				
%RSD area (3 replicates after PIPAC)	11.3 %	7.1 %				
Δ %Area before/after PIPAC (%)	-9.4 %	9.4 %				
HIC						
tr (min)	12.4	17.8				
Proportion of species before PIPAC	5.1 %	94.9 %				
%RSD area (3 replicates before PIPAC)	3.2 %	3.1 %				
Proportion of species after PIPAC	5.3 %	94.7 %				
%RSD area (3 replicates after PIPAC)	7.2 %	9.0 %				
Δ %Area before/after PIPAC (%)	0.1 %	-0.1 %				
RPLC						
tr (min)	4.1	4.4	4.6	5.6	5.9	6
Proportion of species before PIPAC	1.5 %	18.7 %	0.6 %	12.5 %	58.8 %	8.0 %
%RSD area (3 replicates before PIPAC)	3.2 %	3.2 %	3.6 %	3.5 %	3.2 %	2.6 %
Proportion of species after PIPAC	1.5 %	18.8 %	0.5 %	12.5 %	59.1 %	7.6 %
%RSD area (3 replicates after PIPAC)	8.0 %	7.5 %	7.6 %	7.6 %	7.4 %	8.7 %
Δ %Area before/after PIPAC (%)	0.0 %	0.0 %	0.0 %	0.0 %	0.3 %	-0.4 %

40 min), resulting in improved separation as shown in [Figure S1 of the supplementary material](#). A much better resolution of the charge variants was obtained under these conditions and this method confirmed the observed differences in charge variants before and after PIPAC.

Recent analysis of trastuzumab-deruxtecan using CEX coupled with

mass spectrometry (MS) unambiguously identified specific oxidized variants and aspartate isomerization, which are consistent with our observations [16]. Literature also suggests that certain metals like Fe, Cu, Mg, Zn, Mn, Ni, or Co can alter the quality of biotherapeutics by impacting charge variants and aggregate profiles [23]. The CapnoPen® device used in PIPAC, which is a tubing of about 40 cm long used for aerosolization of chemotherapy during PIPAC, is made from nickel and chromium, and might influence the charge variant profile due to its material composition. Although changes in the charge variant profile can be critical for mAbs, they are less impactful for an ADC product from a clinical perspective than changing the variants of the payload, likely not inducing significant changes in efficacy and toxicity.

### 3.3. Analysis of hydrophobicity variants and free payloads using HIC and RPLC

In addition to other analyses, experiments were conducted using RPLC and HIC. These separation techniques are effective in distinguishing hydrophobic variants such as disulfide scrambling and oxidation, which may affect the drug efficacy, safety, and shelf life. The key difference between these two methods is that RPLC operates in a denaturing mode that achieves high efficiency with narrow peaks, whereas HIC operates in a non-denaturing mode. Although HIC exhibits lower efficiency, it offers excellent selectivity for hydrophobicity variants, making it a complementary method to RPLC [24]. HIC is particularly valuable for characterizing ADC products like trastuzumab-deruxtecan, as it provides CQAs such as the average drug-to-antibody ratio (DAR) and the DAR distribution [25]. Trastuzumab-deruxtecan is manufactured using a standard cysteine conjugation approach with a maleimide precursor targeting Cys residues of trastuzumab. The process involves reducing disulfide bonds in the hinge region of trastuzumab and attaching precursor drug linkers to the reduced mAb, resulting in a DAR of 8 with homogeneous conjugation. This process ensures the efficient delivery of the therapeutic payload to target cells [26,27]. In HIC, typically only the main species (DAR 8) is observed due to its non-denaturing conditions. Conversely, under the denaturing conditions of RPLC which is characterized by aggressive mobile phase conditions such as acidic pH, high temperature, and the presence of organic solvents, the ADC sample is denatured. This denaturation, coupled with the absence of interchain disulfide bonds, results in the appearance of two main species in the trastuzumab-deruxtecan sample: a light chain with one cytotoxic drug (L1) and a heavy chain with three cytotoxic drugs (H3).

The chromatograms obtained in RPLC are displayed in Figs. 2–4C, while those in HIC are shown in Figs. 2–4D. In the case of pembrolizumab, RPLC identified four distinct peaks, all eluting within a narrow time window from 5.3 to 5.7 min. In contrast, HIC revealed seven distinct peaks, with elution times ranging from 13.3 to 23.6 min. As detailed in Table 1, the main isoform of pembrolizumab accounts for 95.5 % of the total peak areas in RPLC and 80 % in HIC, highlighting the enhanced selectivity offered by HIC compared to RPLC. When comparing the chromatographic profiles of the three pembrolizumab samples before and after PIPAC treatment, no significant differences were noted in either chromatographic mode. The observed peaks remained consistent (with no new species detected), and the relative amounts of the variants were virtually unchanged in RPLC, showing variations of only up to 0.4 % at most in HIC. This stability confirms that hydrophobicity variants are neither created nor altered during the PIPAC process.

In the analysis of trastuzumab-deruxtecan using HIC, a single hydrophilic variant was clearly separated, and identified as a heavy chain with one cytotoxic drug (H1), according to [16]. At both tested concentrations, the quantities of the variants and the main species remained unchanged before and after PIPAC, as indicated in Tables 2 and 3. However, there was an increased variability in the peak areas post-PIPAC, as noted earlier with other chromatographic modes.

Additionally, naked trastuzumab was injected and eluted at 10.8 min in HIC, distinctly separate from the main isoform DAR 8, which elutes at 17.8 min (data not shown). The HIC profile confirms that there is no change in the average DAR or the DAR distribution, with no new peaks observed between the elution times of DAR 0 (10.8 min) and DAR 8 (17.8 min). This indicates that there is no payload detachment from ADC molecules during PIPAC, an essential consideration given the high off-target toxicity of free payloads and their critical impact on patient safety [28,29].

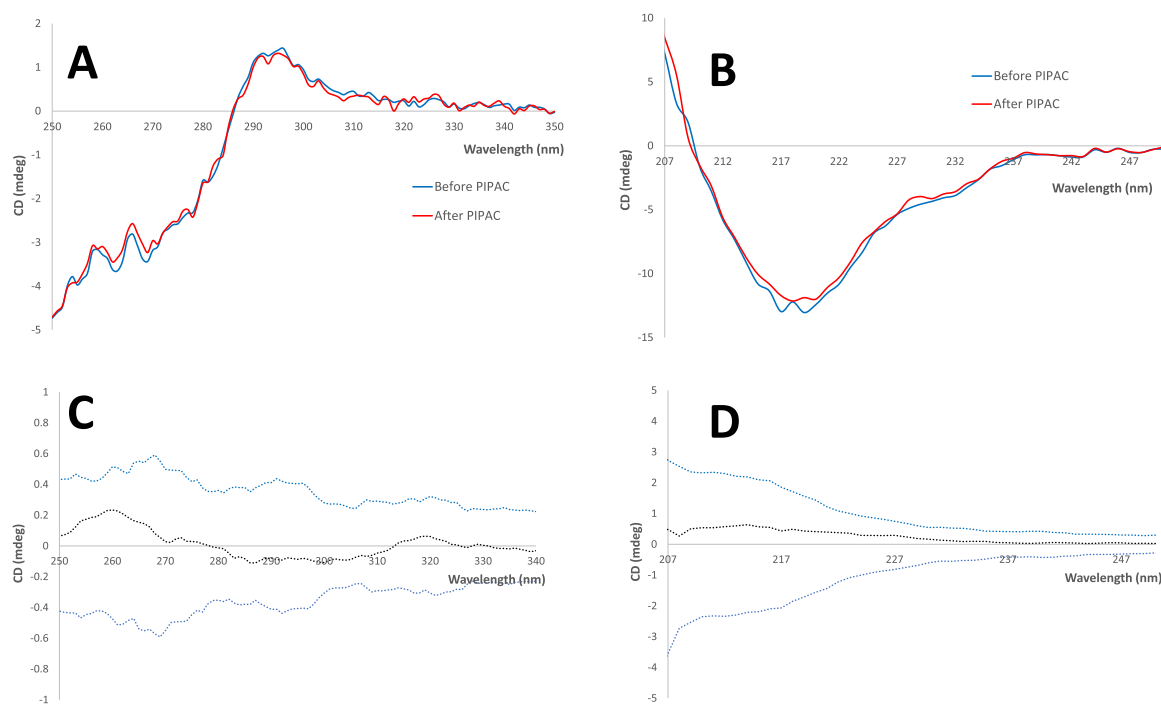
RPLC experiments with trastuzumab-deruxtecan were also conducted and revealed two main species, L1 eluting at 4.4 min and H3 at 5.9 min. Additional peaks near these main species were also noted. According to Desligniere *et al.* [16], these additional peaks likely represent fragmentation within the payload, oxidation, or deamidation. No free light or heavy chains were detected in RPLC, as reduced trastuzumab showed light chains (LC) eluting at 4.2 min and heavy chains (HC) at 5.4 min (data not shown). From Tables 2 and 3, the relative proportions of L1 and H3 were approximately 19 % and 59 %, respectively, indicating a significant presence of hydrophobic variants in the trastuzumab-deruxtecan product. For clarity, the data were categorized into six groups: pre-L1, L1, post-L1, pre-H3, H3, and post-H3 in the two tables. Similar to the HIC findings, the relative quantities of all species remained consistent before and after PIPAC in RPLC, with differences in peak areas ranging between -0.6 % and 0.6 %, confirming that no additional species were created during PIPAC treatment.

### 3.4. Evaluation of the secondary and tertiary structures using CD

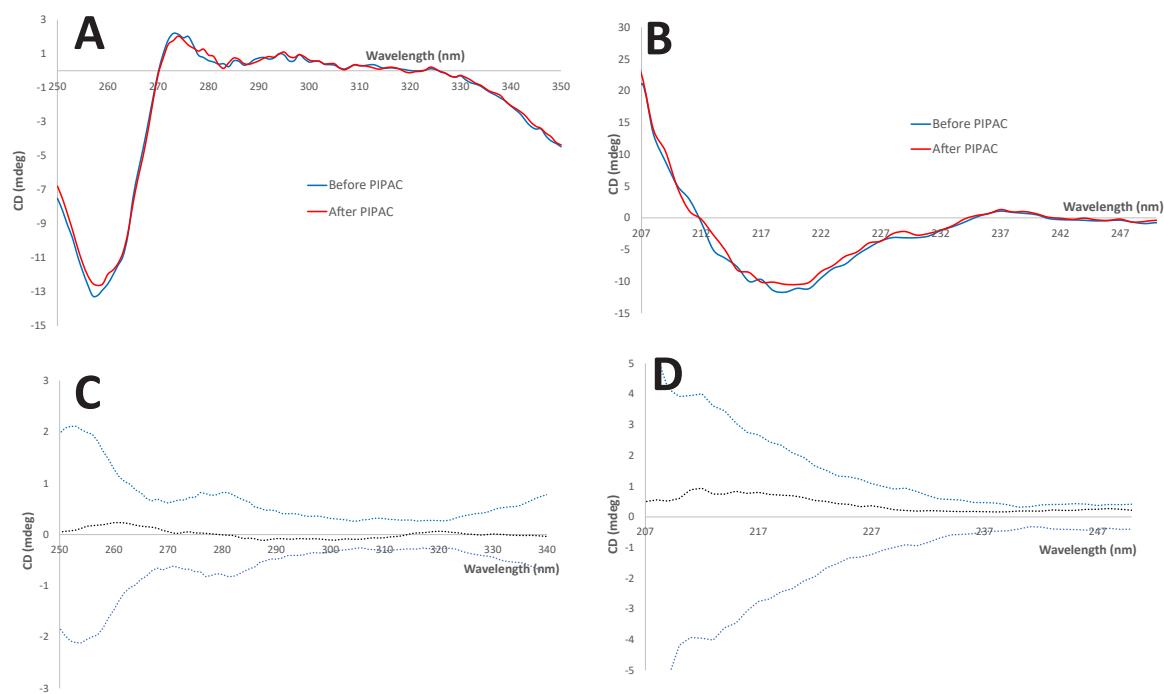
Circular dichroism (CD) spectroscopy was used to examine the higher-order structures (HOS) of pembrolizumab and trastuzumab-deruxtecan before and after PIPAC. This method is favoured for several reasons: it is fast and efficient, non-destructive, highly sensitive to changes in protein conformation, compatible with various buffer systems, and well-supported by regulatory agencies [30,31]. CD spectroscopy has been utilized in over 95 % of biosimilar applications for mAbs and other biotherapeutics [32]. It is critical to recognize that even minor alterations in HOS can significantly impact the biological activity, interactions, stability, and overall efficacy and safety of a biotherapeutic product.

Fig. 5A, 6A and S2A display of the tertiary structures of pembrolizumab and trastuzumab deruxtecan, analyzed in the near-UV range (250–350 nm) to detect signals from tryptophan, tyrosine, and phenylalanine residues. The averaged spectra from three samples analyzed before PIPAC and three samples analyzed after PIPAC were superimposed. While some minor differences were visible between the two sets of averaged spectra, a statistical evaluation suggested these are not indicative of changes in molecule conformation. For a given data point standard deviation was calculated (for both before and after datasets selecting the greater value) and its double (common statistical significance acceptance criteria) was plotted against differential signal of averaged spectra using Figs. 5C, 6C, and S2C. As seen in the figures, the differences were below this threshold, confirming that the tertiary structures of the samples were not altered by PIPAC administration.

This approach was similarly utilized to evaluate the secondary structures, analyzing signals from  $\alpha$ -helices,  $\beta$ -sheets, turns, and random coils within the wavelength range of 205–250 nm. The average spectra before and after PIPAC are depicted in Figs. 5B, 6B, and S2B with the accompanying statistical analyses presented in Figs. 5D, 6D and S2D. In each case, the observed differences between the average spectra before and after PIPAC consistently remained well below the  $\pm 2\sigma$  threshold. This consistently demonstrates that there are no statistically significant differences in the secondary structures of the samples before versus after PIPAC treatment.



**Fig. 5.** Circular dichroism spectra of the pembrolizumab at a concentration of 2 mg/mL. Averaged CD spectra comparison in A) near UV region, (B) far UV region. Differential CD signal obtained before and after PIPAC in C) near UV vs.  $2\sigma$ , D) far UV vs.  $2\sigma$ .



**Fig. 6.** Near and far UV circular dichroism spectra of the trastuzumab-deruxtecan at a concentration of 0.5 mg/mL. (A) Near UV average CD spectrum comparison, (B) Far UV average CD spectrum comparison, (C) Comparison of differences between CD spectra obtained before and after PIPAC in near UV vs.  $2\sigma$ , (D) Comparison of differences between CD spectra obtained before and after PIPAC in far UV vs.  $2\sigma$ .

#### 4. Conclusions

This study provides robust evidence supporting the clinical evaluation of intraperitoneal Keytruda (pembrolizumab) and Enhertu (trastuzumab-deruxtecan), respectively, administered through PIPAC. Extensive pre- and post-PIPAC analyses using various chromatographic

techniques (SEC, IEX, RPLC, and HIC) and spectroscopic methods (UV-CD) have verified that PIPAC maintains the structural and chemical integrity of these advanced biopharmaceutical products throughout the aerosolization process. Importantly, the consistency in size and hydrophobicity variants, along with the average DAR and its distribution, confirms the absence of significant degradation or alteration in the

primary structures of the drugs. The secondary and tertiary structures of the two biopharmaceutical products were not altered, as shown by UV-CD.

Our study identified a non-negligible change in the quantity of charge variants for trastuzumab- deruxtecan after PIPAC application, although this did not alter the type of variants. Given the current understanding of ADC pharmacodynamics, this variation should be further investigated to optimize delivery of this novel precise chemotherapy agent and elucidate the cause and consequences of these differences. The metallic composition of the CapnoPen® device used in PIPAC, which includes nickel and chromium, could possibly explain the observed differences.

In conclusion, our results suggest that PIPAC does not alter the structure of these two breakthrough anti-cancer agents which could hence be administered directly within the peritoneal cavity, preserving their efficacious structure. Our study paves the way for future innovative clinical trials investigating immunotherapy and ADCs to treat patients with peritoneal carcinomatosis, a hard to treat and unmet need in oncology.

### CRedit authorship contribution statement

**Laurent Carrez:** Writing – review & editing, Resources, Methodology, Investigation, Funding acquisition, Conceptualization. **Davy Guillaume:** Writing – review & editing, Writing – original draft, Validation, Supervision, Resources, Project administration, Methodology, Conceptualization. **Valentina D'Atri:** Writing – review & editing, Visualization, Formal analysis, Data curation. **Guillaume Galy:** Writing – review & editing, Methodology, Investigation, Conceptualization. **Mathias Buff:** Formal analysis, Data curation. **Mateusz Imiolek:** Writing – review & editing, Visualization, Formal analysis, Data curation. **Martin Hübner:** Writing – review & editing, Methodology, Investigation, Conceptualization. **Manuela Undurraga:** Writing – review & editing, Methodology, Investigation, Conceptualization. **Sana Intidhar Labidi-Galy:** Writing – review & editing, Resources, Funding acquisition, Conceptualization.

### Declaration of Competing Interest

The authors declare the following financial interests/personal relationships which may be considered as potential competing interests. The authors declare the following competing financial interests: Mateusz Imiolek is an employee of Waters (Milford, MA, USA), a manufacturer of chromatography systems and consumables. ACQUITY, UPLC, Empower and BioResolve are trademarks of Waters Technologies Corporation. Capnopen® is a trademark of Capno pharm GmbH. Milli-Q is a trademark of Merck KGaA. Keytruda is a trademark of Merck Sharp & Dohme, LLC. Enhertu is a trademark of Daiichi Sankyo Company Limited. Accutron is a trademark of Medtron AG. AdvanceBio is a trademark of Agilent Technologies Inc. MABPac is a trademark of Thermo Fisher Scientific AG. Excel is a trademark of Microsoft Corporation. All other trademarks are the property of their respective owners.

### Acknowledgements

We extend our gratitude to the operating room team at Lausanne University Hospital for their invaluable support throughout this study, specifically to Mrs Caroline Delgrange, Mrs Marija Bogdanovic, Mrs Miria Ciavatta, Mrs Joana Cajao-Oliveira and Mr Ahmed Ait Benamara for sharing their expertise that was crucial to the success of this research project.

### Appendix A. Supporting information

Supplementary data associated with this article can be found in the online version at [doi:10.1016/j.jpba.2024.116410](https://doi.org/10.1016/j.jpba.2024.116410).

### References

- [1] D. Cortés-Guiral, M. Hübner, M. Alyami, A. Bhatt, W. Ceelen, O. Glehen, F. Lordick, R. Ramsay, O. Sgarbura, K. Van Der Speeten, K.K. Turaga, M. Chand, Primary and metastatic peritoneal surface malignancies, *Nat. Rev. Dis. Prim.* 7 (2021) 91, <https://doi.org/10.1038/s41572-021-00326-6>.
- [2] M. Alyami, M. Hübner, F. Grass, N. Bakrin, L. Villeneuve, N. Laplace, G. Passot, O. Glehen, V. Kepenian, Pressurised intraperitoneal aerosol chemotherapy: rationale, evidence, and potential indications, *Lancet Oncol.* 20 (2019) e368–e377, [https://doi.org/10.1016/S1470-2045\(19\)30318-3](https://doi.org/10.1016/S1470-2045(19)30318-3).
- [3] M. Hübner, F. Grass, H. Teixeira-Farinha, B. Pache, P. Mathevet, N. Demartines, Pressurised IntraPeritoneal aerosol chemotherapy – practical aspects, *Eur. J. Surg. Oncol. EJSO* 43 (2017) 1102–1109, <https://doi.org/10.1016/j.ejso.2017.03.019>.
- [4] M. Borgeaud, J. Sandoval, M. Obeid, G. Banna, O. Michielin, A. Addeo, A. Friedlaender, Novel targets for immune-checkpoint inhibition in cancer, *Cancer Treat. Rev.* 120 (2023) 102614, <https://doi.org/10.1016/j.ctrv.2023.102614>.
- [5] C. Dumontet, J.M. Reichert, P.D. Senter, J.M. Lambert, A. Beck, Antibody–drug conjugates come of age in oncology, *Nat. Rev. Drug Discov.* 22 (2023) 641–661, <https://doi.org/10.1038/s41573-023-00709-2>.
- [6] M.S. Kim, V. Prasad, Pembrolizumab for all, *J. Cancer Res. Clin. Oncol.* 149 (2023) 1357–1360, <https://doi.org/10.1007/s00432-022-04412-4>.
- [7] A. Goyon, V. D'Atri, B. Bobaly, E. Wagner-Rousset, A. Beck, S. Fekete, D. Guillaume, Protocols for the analytical characterization of therapeutic monoclonal antibodies. I – Non-denaturing chromatographic techniques, *J. Chromatogr. B* 1058 (2017) 73–84, <https://doi.org/10.1016/j.jchromb.2017.05.010>.
- [8] C. Nowak, J. K. Cheung, S. M. Dellatore, A. Katiyar, R. Bhat, J. Sun, G. Ponniah, A. Neill, B. Mason, A. Beck, H. Liu, Forced degradation of recombinant monoclonal antibodies: a practical guide, *mAbs* 9 (2017) 1217–1230, <https://doi.org/10.1080/19420862.2017.1368602>.
- [9] S. Fekete, A. Beck, J.-L. Veuthey, D. Guillaume, Theory and practice of size exclusion chromatography for the analysis of protein aggregates, *J. Pharm. Biomed. Anal.* 101 (2014) 161–173, <https://doi.org/10.1016/j.jpba.2014.04.011>.
- [10] V. D'Atri, M. Imiolek, C. Quinn, A. Finny, M. Lauber, S. Fekete, D. Guillaume, Size exclusion chromatography of biopharmaceutical products: From current practices for proteins to emerging trends for viral vectors, nucleic acids and lipid nanoparticles, *J. Chromatogr. A* 1722 (2024) 464862, <https://doi.org/10.1016/j.chroma.2024.464862>.
- [11] A. Goyon, S. Fekete, A. Beck, J.-L. Veuthey, D. Guillaume, Unraveling the mysteries of modern size exclusion chromatography – the way to achieve confident characterization of therapeutic proteins, *J. Chromatogr. B* 1092 (2018) 368–378, <https://doi.org/10.1016/j.jchromb.2018.06.029>.
- [12] A. Murisier, M. Andrie, S. Fekete, M. Lauber, V. D'Atri, K. Iwan, D. Guillaume, Direct coupling of size exclusion chromatography and mass spectrometry for the characterization of complex monoclonal antibody products, *J. Sep. Sci.* 45 (2022) 1997–2007, <https://doi.org/10.1002/jssc.202200075>.
- [13] A. Murisier, S. Fekete, D. Guillaume, V. D'Atri, The importance of being metal-free: The critical choice of column hardware for size exclusion chromatography coupled to high resolution mass spectrometry, *Anal. Chim. Acta* 1183 (2021) 338987, <https://doi.org/10.1016/j.aca.2021.338987>.
- [14] A. Goyon, A. Beck, J.-L. Veuthey, D. Guillaume, S. Fekete, Comprehensive study on the effects of sodium and potassium additives in size exclusion chromatographic separations of protein biopharmaceuticals, *J. Pharm. Biomed. Anal.* 144 (2017) 242–251, <https://doi.org/10.1016/j.jpba.2016.09.031>.
- [15] A. Ehkirch, A. Goyon, O. Hernandez-Alba, F. Rouviere, V. D'Atri, C. Dreyfus, J.-F. Haeuw, H. Diemer, A. Beck, S. Heinisch, D. Guillaume, S. Cianferani, A novel online four-dimensional SEC×SEC-IM×MS methodology for characterization of monoclonal antibody size variants, *Anal. Chem.* 90 (2018) 13929–13937, <https://doi.org/10.1021/acs.analchem.8b03333>.
- [16] E. Deslignière, H. Diemer, S. Erb, P. Coliat, X. Pivot, A. Detappe, O. Hernandez-Alba, S. Cianferani, A combination of native LC-MS approaches for the comprehensive characterization of the antibody–drug conjugate trastuzumab deruxtecan, *Front. Biosci. -Landmark* 27 (2022) 290, <https://doi.org/10.31083/j.fbl2710290>.
- [17] L.A. Khawli, S. Goswami, R. Hutchinson, Z.W. Kwong, J. Yang, X. Wang, Z. Yao, A. Sreedhara, T. Cano, D.B. Tesar, I. Nijem, D.E. Allison, P.Y. Wong, Y.-H. Kao, C. Quan, A. Joshi, R.J. Harris, P. Motchnik, Charge variants in IgG1: isolation, characterization, in vitro binding properties and pharmacokinetics in rats, *mAbs* 2 (2010) 613–624, <https://doi.org/10.4161/mabs.2.6.13333>.
- [18] J. Vlasak, R. Ionescu, Heterogeneity of monoclonal antibodies revealed by charge-sensitive methods, *Curr. Pharm. Biotechnol.* 9 (2008) 468–481, <https://doi.org/10.2174/138920108786786402>.
- [19] Y. Du, A. Walsh, R. Ehrick, W. Xu, K. May, H. Liu, Chromatographic analysis of the acidic and basic species of recombinant monoclonal antibodies, *mAbs* 4 (2012) 578–585, <https://doi.org/10.4161/mabs.21328>.
- [20] A. Goyon, M. Excoffier, M.-C. Janin-Bussat, B. Bobaly, S. Fekete, D. Guillaume, A. Beck, Determination of isoelectric points and relative charge variants of 23 therapeutic monoclonal antibodies, *J. Chromatogr. B* 1065–1066 (2017) 119–128, <https://doi.org/10.1016/j.jchromb.2017.09.033>.
- [21] S. Fekete, A. Beck, J.-L. Veuthey, D. Guillaume, Ion-exchange chromatography for the characterization of biopharmaceuticals, *J. Pharm. Biomed. Anal.* 113 (2015) 43–55, <https://doi.org/10.1016/j.jpba.2015.02.037>.
- [22] P. Sundaramurthi, S. Chadwick, C. Narasimhan, Physicochemical stability of pembrolizumab admixture solution in normal saline intravenous infusion bag, *J. Oncol. Pharm. Pract.* 26 (2020) 641–646, <https://doi.org/10.1177/1078155219868516>.

- [23] N. Gangwar, R. Mishra, N. Budholiya, A.S. Rathore, Effect of vitamins and metal ions on productivity and charge heterogeneity of IgG1 expressed in CHO cells, *Biotechnol. J.* 16 (2021) 2000464, <https://doi.org/10.1002/biot.202000464>.
- [24] S. Fekete, J.-L. Veuthey, A. Beck, D. Guilleme, Hydrophobic interaction chromatography for the characterization of monoclonal antibodies and related products, *J. Pharm. Biomed. Anal.* 130 (2016) 3–18, <https://doi.org/10.1016/j.jpba.2016.04.004>.
- [25] R. Fleming, ADC analysis by hydrophobic interaction chromatography, in: L. N. Tumey (Ed.), *Antib.-Drug Conjug.*, Springer US, New York, NY, 2020, pp. 147–161, [https://doi.org/10.1007/978-1-4939-9929-3\\_10](https://doi.org/10.1007/978-1-4939-9929-3_10).
- [26] T. Nakada, T. Masuda, H. Naito, M. Yoshida, S. Ashida, K. Morita, H. Miyazaki, Y. Kasuya, Y. Ogitani, J. Yamaguchi, Y. Abe, T. Honda, Novel antibody drug conjugates containing exatecan derivative-based cytotoxic payloads, *Bioorg. Med. Chem. Lett.* 26 (2016) 1542–1545, <https://doi.org/10.1016/j.bmcl.2016.02.020>.
- [27] G.D. Lewis Phillips, G. Li, D.L. Dugger, L.M. Crocker, K.L. Parsons, E. Mai, W. A. Blättler, J.M. Lambert, R.V.J. Chari, R.J. Lutz, W.L.T. Wong, F.S. Jacobson, H. Koeppen, R.H. Schwall, S.R. Kenkare-Mitra, S.D. Spencer, M.X. Sliwkowski, Targeting HER2-Positive Breast Cancer with Trastuzumab-DM1, an antibody–cytotoxic drug conjugate, *Cancer Res* 68 (2008) 9280–9290, <https://doi.org/10.1158/0008-5472.CAN-08-1776>.
- [28] F. Yin, D. Adhikari, Y. Li, D. Turner, M. Shane Woolf, D. Lebarbenchon, E. Ma, W. Mylott, E. Shaheen, S. Harriman, J. Pinkas, A sensitive and rapid LC-MS/MS assay for quantitation of free payload Aur0101 from antibody drug conjugate (ADC) PYX-201 in human plasma, *J. Chromatogr. B* 1226 (2023) 123786, <https://doi.org/10.1016/j.jchromb.2023.123786>.
- [29] P. Tarantino, B. Ricciuti, S.M. Pradhan, S.M. Tolaney, Optimizing the safety of antibody–drug conjugates for patients with solid tumours, *Nat. Rev. Clin. Oncol.* 20 (2023) 558–576, <https://doi.org/10.1038/s41571-023-00783-w>.
- [30] L.A. Linhares, C.H.I. Ramos, Unlocking insights into folding, structure, and function of proteins through circular dichroism spectroscopy—a short review, *Appl. Biosci.* 2 (2023) 639–655, <https://doi.org/10.3390/applbiosci2040040>.
- [31] A.J. Miles, R.W. Janes, B.A. Wallace, Tools and methods for circular dichroism spectroscopy of proteins: a tutorial review, *Chem. Soc. Rev.* 50 (2021) 8400–8413, <https://doi.org/10.1039/D0CS00558D>.
- [32] D. Marshall, Optimizing circular dichroism spectroscopy: provides key information on changes in secondary and tertiary structure of proteins, *Genet. Eng. Biotechnol.* N. 38 (2018) 20–21, <https://doi.org/10.1089/gen.38.10.07>.